Universität Zürich[UZH]

Decomposition of the Hadronic Tensor up to Spin 2

Bachelor Thesis in Physics

Marvin Sigg

Supervised by
Prof. Dr. Adrian Signer

August 2024

Abstract

We closely examine the transition amplitude of elastic scattering of leptons off various heavy hadron targets in the one-photon-exchange approximation. While the term of the hadron can be handled at leading order, the much more dominant contribution of the lepton is currently being studied at next-to-next-to-leading order. The calculation of the amplitude squared, consisting of the leptonic and hadronic part, is therefore increasingly complicated.

This thesis aims to separate the two contributions for much simpler computations when selecting a new hadron as the target. The central mathematical variations are arising from the differing spins of the hadron targets, which we are discussing up to and including spin 2.

Acknowledgements

First and foremost I want to express my gratitude to Adrian for this opportunity, his patience, and infectious enthusiasm. You always inspired me, and I learned way more than how to write a thesis. I am very grateful for the McMule subgroup: Sophie, Marco, Daniel, David, and Sara. Thank you for your constant and patient support and many insightful discussions. In general, I want to thank the whole LTP Theory Group at PSI for a welcoming atmosphere. Thank you to Ennio, Urs, and Philipp for proofreading my drafts. Finally, I want to warmly thank my family for their love and support in many different ways.

To my aunt Regine, who supported me in many invaluable ways.

Contents

1 Introduction

A century ago, quantum mechanics shook the foundation of physics and our understanding of reality. It emerged from the first quantisation, which converted classical particle equations into quantum wave equations. The second quantisation gave rise to quantum field theory, which converted classical field equations into quantum field equations.

The scientific developments in the early 20th century culminated in the formulation of the Standard Model of particle physics (SM) in the 1970s. The SM has proven time and again to be an exceptionally accurate theory. Quantum electrodynamics (QED) is an important subfield of study, and efforts both theoretical and experimental persist to this day.

1.1 Experimental preface

To highlight practical endeavours in the precision frontier, consider the measurements performed at the Mainz Microtron (MAMI) in 2013 [1]. They are focused on resolving the proton radius puzzle, which describes the discrepancy between the measurements of the proton radius through established methods and more recent procedures involving exotic atoms such as muonic hydrogen [2]. The novelty in their traditional approach of electron-proton scattering lies in the minimal energy transfer, which allows for precise measurements.

While the proton radius puzzle describes important fundamental research, the proposed targets are not limited to protons. A second, very recent development is the emerging ULQ2 (Ultra-Low Q2) spectrometer experiment [3] at the Tohoku University. This facility, too, is concerned with low-energy electron scattering, and intends to measure the charge radius of the deuterium and carbon nucleus, amongst other things.

1.2 Motivation and McMule

McMule (Monte Carlo for MUons and other LEptons) is an open-source framework to perform QED calculations of scattering and decay processes involving leptons. In particular, it employs Monte Carlo integration to calculate differential cross sections up to next-to-next-to-leading order (NNLO) [4]. The emphasis is thus set on precision physics. Here, we focus on elastic scattering processes of the form

$$X(p_i) + l(k_i) \to X(p_f) + l(k_f)\,, \tag{1}$$

where l designates the lepton and X the arbitrary hadronic target, which an atomic nucleus in most cases.

As part of preparing a computation, we have to "feed" the Mule information regarding the particles. The required input includes the squared transition amplitude associated with the scattering process. A key factor there is to obtain special functions called form factors from the literature. They correspond to the electromagnetic charge distribution of the particles. The output, in that case, is the differential cross section, which is a measure of the probability of a scattering process.

An important consideration is the bremsstrahlung, where a charged particle experiences deceleration upon deflection by another charged particle. This converts some of the kinetic energy of the decelerated charged particle into electromagnetic radiation. Due to their small relative mass compared to hadrons, leptons experience a much stronger deceleration than hadrons and their contributions to radiation are therefore overwhelmingly dominant compared to hadrons.

For this reason, the mathematical expression of leptons must incorporate NNLO corrections. For hadrons, leading order (LO) suffices in most cases. This is indicated visually in the Feynman diagram in Figure 1.

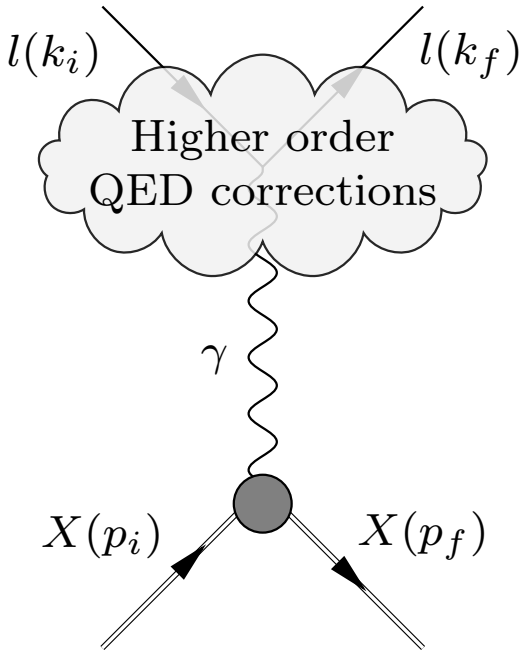

Figure 1: Feynman diagram of the elastic scattering of leptons off hadron targets in the one-photon-exchange approximation, $X(p_i) + l(k_i) \to X(p_f) + l(k_f)$.

The diagram illustrates how the hadrons, despite their complex inner making, are well understood at low energy scales in LO. The leptons on the other hand, which are simple, fundamental particles, yield very complicated terms at NNLO. To get a sense of the complexity of the expressions of leptons at higher order, check out [5]. The cloud shape indicates that these expressions are not of our interest in this thesis.

Currently, one has to cumbersomely repeat the calculation of the amplitude, which is fed into McMule, for every new hadronic target. The complication arises due to the intricate terms at NNLO associated with the lepton.

This thesis aims to consider a new approach in calculation. In particular, we discuss the mathematical challenges and consequences of the new strategy and provide baseline calculations in both analytical and numerical territory.

2 General procedure

2.1 Analytical ansatz

Consider the one-photon-exchange approximation of the scattering of a lepton off a target hadron. Ignoring prefactors, the amplitude can be written as

$$\mathcal{M} = j^\mu J_\mu \,. \tag{2}$$

From there, we isolate the electromagnetic four-current J^μ, which describes the transition between the initial and the final state of the target, while j^μ is associated with the lepton. The four-current is generally defined as

$$J^\mu = \langle \psi_f | \Gamma | \psi_i \rangle^\mu \,, \tag{3}$$

where Γ denotes the vertex and ψ a suitable wave function, i indicating the initial and f the final state. J^μ is the relativistic equivalent of the charge density, which describes the amount of charge per time passing through a unit cross section.

The structure of Γ and ψ varies from particle to particle, but we know that J^μ is a vector in the Lorentz space. It obeys the continuity equation

$$\partial_\mu J^\mu = 0 \,, \tag{4}$$

which simply states that the charge is locally conserved. By shifting the continuity equation from the position space into the momentum space, we obtain the requirement

$$q_\mu \langle \psi_f | \Gamma | \psi_i \rangle^\mu \stackrel{!}{=} 0 \,, \tag{5}$$

where $q = p_f - p_i$ denotes the four-momentum transfer. This is a useful mechanism to derive the makeup of Γ.

The mathematical structure of the wave functions, both in the Lorentz space and the spinor space, is highly dependent on the spin. The structure of the vertex must change accordingly to harmonise with ψ, which from now on only represents the spin-dependent part of the wave function.

In general, the spin function of a particle with intrinsic spin j yields $\lfloor j \rfloor$ Lorentz indices. Therefore, Γ must possess $2\lfloor j \rfloor + 1$ Lorentz indices which contract to a single index when the two spin functions are applied,

$$J^\mu = (\bar{\psi}_f)_{\nu_1 \dots \nu_{\lfloor j \rfloor}} \Gamma^{\mu \nu_1 \dots \nu_{\lfloor j \rfloor} \rho_1 \dots \rho_{\lfloor j \rfloor}} (\psi_i)_{\rho_1 \dots \rho_{\lfloor j \rfloor}} \,. \tag{6}$$

Once the current has been obtained, we form the hadronic tensor

$$H_{\mu\nu} = J_\mu J_\nu^\dagger \,. \tag{7}$$

The leptonic tensor $L^{\mu\nu}$ is defined similarly. Take note: this tensor is still implicitly spin-dependent. However, most experiments do not differ between different spin states.

To mitigate this dependency, we sum over all helicity state combinations of the incoming and outgoing hadron, averaging over the $2j+1$ possible initial states,

$$H_{\mu\nu}^{(0)} = \frac{1}{2j+1}\Big(\sum_{\text{spin out}}\sum_{\text{spin in}} H_{\mu\nu}\Big)\,. \tag{8}$$

We call this tensor unpolarised and mark it with a (0). Since the spinors reappear in the explicit helicity sum, we must carefully differentiate between different scattering targets regarding their spin j, which must be reflected in their representation.

In practice, the hadronic targets are mostly nuclei. Their rule of thumb is:

- Odd mass nuclei have fractional spins (j is a half-integer).
- Even mass nuclei composed of odd numbers of protons and neutrons have integral spins (j is an integer).
- Even mass nuclei composed of even numbers of protons and neutrons have zero spin ($j = 0$).

As a further complication, all nuclei with non-zero spins have magnetic moments, and nuclei with $j \geq 1$ also have an electric quadrupole moment. However, all nuclei possess an electric monopole. Arbitrarily high spins result in arbitrary electromagnetic multipoles, which will be reflected in the form factors present in the current and tensor associated with the hadron. In 1966, Theis stated a method [6] to construct $2j+1$ form factors for spin j.

The next step is to form the unpolarised, squared amplitude which is a measure of the transition probability. Notice that there are generally two ways to compute this,

$$\begin{aligned}\langle|\mathcal{M}|^2\rangle = H_{\mu\nu}^{(0)}L^{(0)\mu\nu} &= \frac{1}{2(2j+1)}\Big(\sum_{\text{spins}} H_{\mu\nu}\Big)\Big(\sum_{\text{spins}} L^{\mu\nu}\Big)\\ &= \frac{1}{2(2j+1)}\sum_{\text{spins}}\big(j^\mu J_\mu\big)\big(j^\nu J_\nu\big)^\dagger = \frac{1}{2(2j+1)}\sum_{\text{spins}}\mathcal{M}\mathcal{M}^\dagger\,.\end{aligned} \tag{9}$$

Figure 2 provides a visual intuition of the two different approaches. Currently, amplitudes are calculated by analytically computing the hadronic and leptonic tensors, which leads to an omission of the explicit representation of the spin functions. This is generally an involved process, as the leptonic expressions at NNLO are very convoluted.

In contrast, future applications of McMule will only require the electromagnetic currents of the particles. The squared amplitude is then calculated via a numerical contraction of the currents, which results in a significantly faster computation. This means that new hadronic targets can get implemented at almost no additional expenditure.

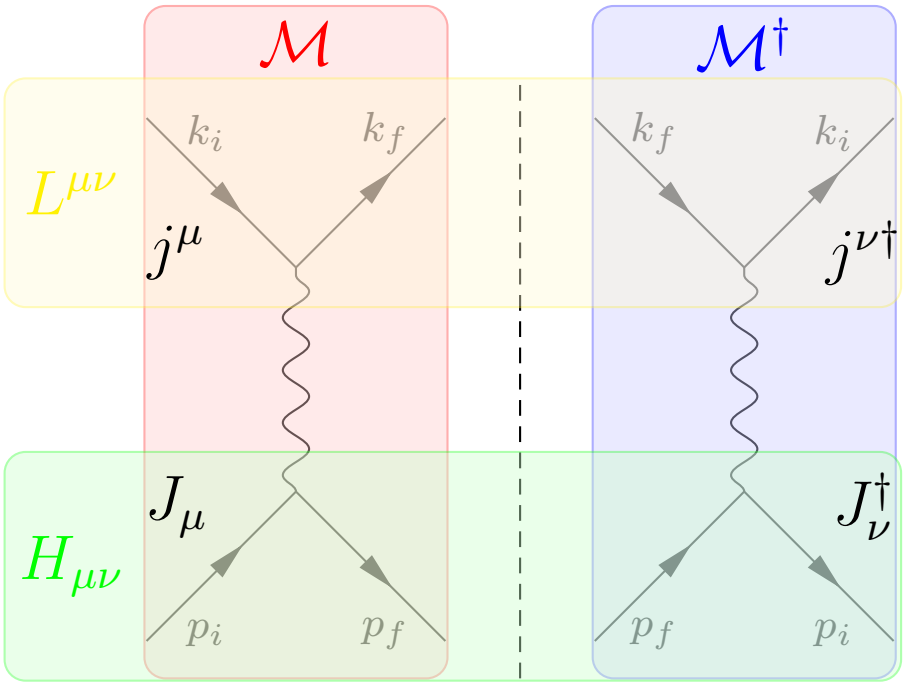

Figure 2: The two different ways of separating the squared amplitude.

2.2 Numerical check

Mathematica was employed for analytical derivations and comprehensive numerical cross-checks. To manage Lorentz indices and compute traces, we used Package-X [7, 8].

The equalities stated here have been checked numerically with many different parameters. In this thesis, we illustrate this using the arbitrary initial and final momentum

$$\begin{aligned} p_i &= \left(\sqrt{5^2+5^2+1^2+7^2}, -5, 1, -7\right) \quad \text{and} \\ p_f &= \left(\sqrt{5^2+4^2+2^2+6^2}, 4, -2, -6\right), \end{aligned} \tag{10}$$

where both the incoming and outgoing hadron have a squared mass of $m^2 = p_i^2 = p_f^2 = 25$. We call particles that satisfy this equality to be on shell. The scalar product is to be understood under the Minkowski metric with signature $(+,-,-,-)$.

Furthermore, form factors are set to 1 in numerical testing for simplicity reasons. For every spin configuration, we compare the traditional procedure which omits the spin functions against the explicit formulation of the spin sum. In the latter case, we must decide on a basis and representation of the spin functions, which will be discussed case by case. The notebooks are available on Github under
https://github.com/MarvinSigg/hadronictensor.

3 Spin 0

As an introductory case, consider spin 0. The prototypical example of a hadron with spin 0 is the carbon ^{12}C nucleus. Its behaviour and form factor are well understood, and it is therefore to this day a prime candidate to probe new precision barriers. [9]

3.1 Derivation of the current

We will now illustrate the procedure discussed in Chapter 2.1. In the trivial case of spin 0, the notion of a spin function is nonsensical. We may therefore express the "spinors" as a 1, which is why we label spin 0 as the scalar case. This leaves not a lot for our vertex to work with.

The only allowed non-trivial Lorentz objects are the initial and final momentum of the carbon nucleus. For J^μ to transform as a Lorentz-vector, only linear combinations of those objects are admitted. Our most general vertex is thus of the form

$$\Gamma^\mu = Ap_i^\mu + Bp_f^\mu \,, \tag{11}$$

where A and B are unknown scalar quantities.

By Equation (5) we require

$$q_\mu(Ap_i^\mu + Bp_f^\mu) = (A-B)(p_i \cdot p_f - m^2) \stackrel{!}{=} 0 \,, \tag{12}$$

and obtain the equality $A = B \equiv F$. The remaining coefficient is scalar, and the only non-trivial scalar appearing is Q^2, which is minus the square of the momentum transfer,

$$Q^2 \equiv -q^2 = -(p_f - p_i)^2 \,. \tag{13}$$

Therefore, we have a single unknown function F depending on Q^2, which is our form factor. Our current takes the form

$$J_\mu = P_\mu F(Q^2) \,, \tag{14}$$

where we abbreviated the momentum sum as

$$P_\mu = (p_i + p_f)_\mu \,. \tag{15}$$

Since there is only one spin configuration in the scalar case, summing over the helicity is superfluous. The hadronic tensor takes the form

$$H^{(0)}_{\mu\nu} = P_\mu P_\nu F(Q^2)^2 \,. \tag{16}$$

Numerically, we evaluate the tensor as

$$H^{(0)}_{\mu\nu} = \begin{pmatrix} 361 & 56 & 80 & 8 \\ 56 & 1 & -35 & 33 \\ 80 & -35 & 1 & 45 \\ 8 & 33 & 45 & 169 \end{pmatrix} . \tag{17}$$

3.2 $^{12}C + e^- \to {}^{12}C + e^- + \gamma$ with McMule

To highlight a practical example of our discussion, let us shift our attention towards the closely related process

$$^{12}C + e^- \to {}^{12}C + e^- + \gamma\,, \tag{18}$$

where the γ describes the emission of a photon. This process was measured at the MAMI by the A1-Collaboration, described in [1, 9] and recently simulated by McMule. The numerical contraction of the tensors required significant changes in OpenLoops [10, 11], which were implemented by Zoller. We show several results of this simulation to link the theoretical examinations with practical considerations.

To accurately simulate the measurements performed, we need to mirror the parameters of the experiment as the input into McMule. The electron beam energy in the lab frame totals $E_{\text{beam}} = 195$ MeV, which translates to a momentum transfer of $Q^2 = 1.29 \times 10^8$ MeV^2, while the carbon is at rest. Because of the experimental setup, the detection of outgoing electrons is confined to a scattering angle of $\theta_e \in [13°, 17°]$. While the scattering angle of the carbon in the experiment was limited as well, the simulation was able to calculate over the whole range of the scattering angle. The scattering angle is generally measured from the axis of the incoming electron beam. Another constraint in parameters is a minimum difference in energy of the outgoing electron of $E_e^{\text{elastic}} - E_e > 61$ MeV compared to elastic scattering without photon emission ($^{12}C + e^- \to {}^{12}C + e^-$). This can be viewed as a measure of the inelasticity of the process. Naturally, the lost energy contributes to the emitted photon.

This $2 \to 3$ process is currently calculated by McMule at next-to-leading order (NLO). At leading order, the total cross section was calculated to be $\sigma_0 = 12.7723(6)$ μb. Including NLO corrections, the value increases to $\sigma_1 = 12.9064(6)$ μb, which is a difference of $K = 1.050(6)\%$. The corrections can be observed in Figures 3, 4 and 5 as the dotted contribution in the upper half. The K-value in the lower half of the figures describes the relative difference between LO and NLO calculations.

The three plots illustrate different dependencies of the differential cross section. This in turn can be used to deduce the most likely physical configurations of the particles after the scattering. For instance, the dependency within the range of the scattering angle of the electron in Figure 3 indicates a trend towards smaller angles. In contrast, Figure 4 shows a strong preference for the scattering angle of the carbon to be roughly perpendicular to the incoming beam.

The plot in Figure 5 reveals the tendency of the electron to lose as much energy to the momentum of the carbon and the radiation as possible. In this plot, a hard cut-off can be observed at around 135 MeV, which is a consequence of the constraining parameters given above.

We will return to the land of the firmly mathematical in the following chapter, but this detour shows the practical goal of theoretical considerations, such as those presented in this thesis. Thanks to the new approach, the spin 0 carbon can be exchanged with any other hadronic target to repeat the calculation with significantly less extra effort than before.

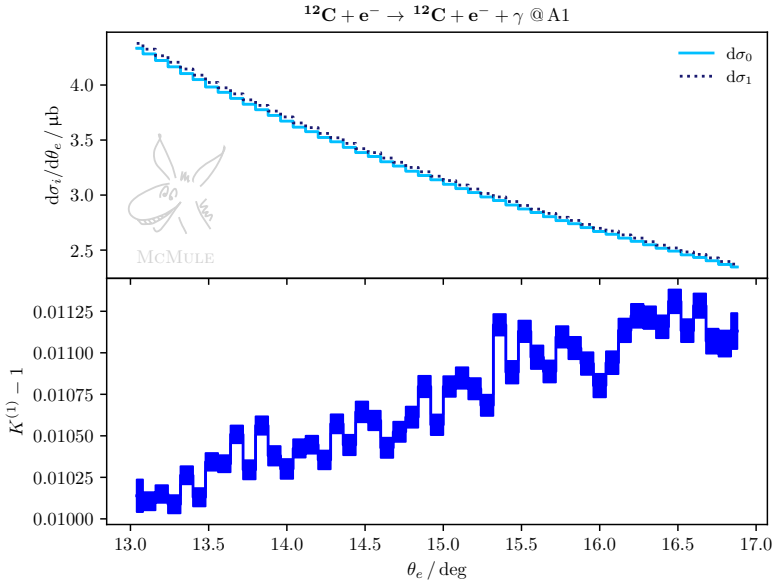

Figure 3: Simulation of the differential cross section depending on the scattering angle $\theta_e \in [13°, 17°]$ of the outgoing electron.

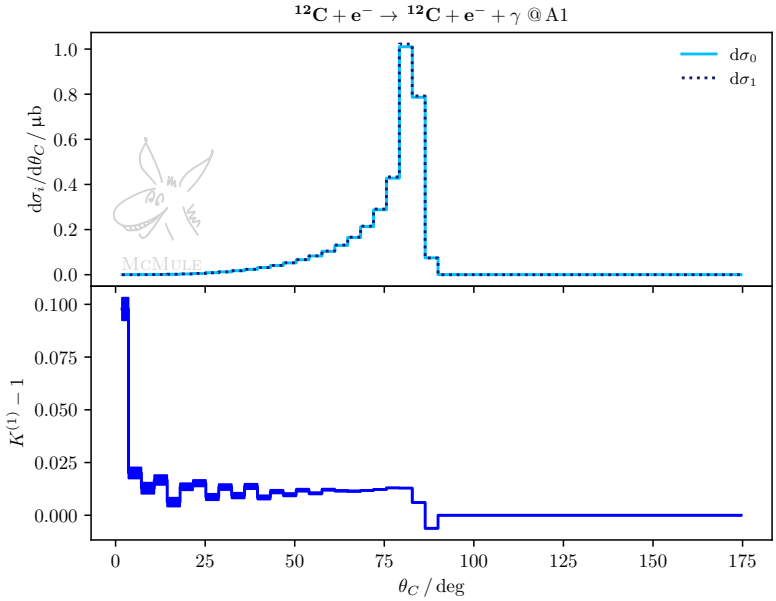

Figure 4: Simulation of the differential cross section depending on the scattering angle θ_C of the outgoing carbon.

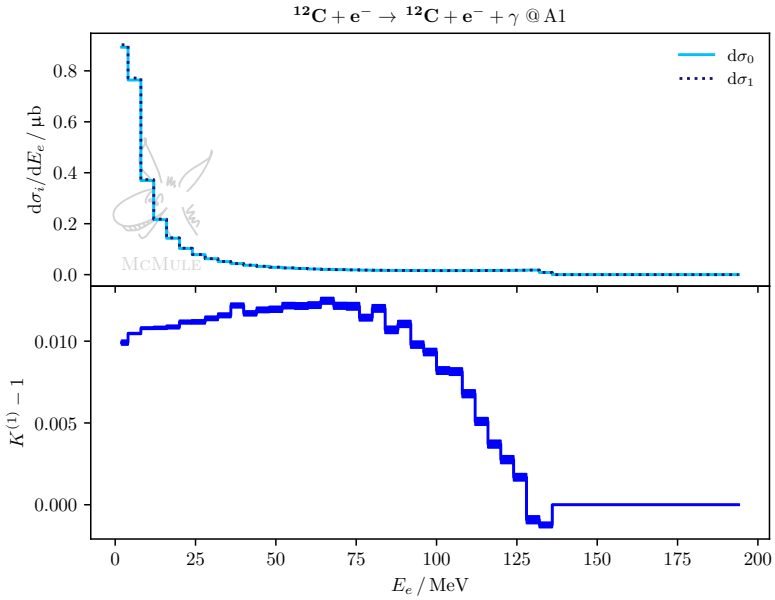

Figure 5: Simulation of the differential cross section depending on the energy of the outgoing electron.

4 Spin 1/2

Many famous particles have intrinsic spin 1/2, including the building blocks of atomic matter. The mathematics behind them is therefore well understood. We inspect the electron and the proton in two separate cases, as their respective charge distributions differ quite drastically from each other.

4.1 The Dirac spinor

To encapsulate the behaviour of spin 1/2-particles accurately, we need suitable mathematical elements which satisfy the Dirac equation

$$(\not{p} - m)u = 0\,, \tag{19}$$

where the slash notation denotes the scalar product of the momentum p with the γ-matrices. The γ-matrices grant us a covariant formulation of the Dirac equation with respect to the Lorentz group. They are a set of four spinor matrices $\{\gamma^0, \gamma^1, \gamma^2, \gamma^3\}$ which must satisfy the Dirac algebra

$$\{\gamma^\mu, \gamma^\nu\} = 2g^{\mu\nu}\,. \tag{20}$$

While the γ-matrices are characterised by their anti-commutativity relations, their commutativity appears often enough to receive a special notation,

$$\sigma^{\mu\nu} = \frac{i}{2}[\gamma^\mu, \gamma^\nu]\,. \tag{21}$$

The common γ^5-matrix is of no use to us. Its implementation is not allowed in our case study, since we require conservation of parity (which γ^5 violates).

The objects solving the Dirac equation are the Dirac spinors u. It should be stressed that, while they are vectors in the spinor space, they are most definitely not in the Lorentz space. The Dirac spinors fulfil the completeness relation

$$\sum_{\lambda=\pm 1/2} u^\lambda \bar{u}^\lambda = \not{p} + m\,, \tag{22}$$

where the "bar" denotes the Dirac adjoint,

$$\bar{u} = u^\dagger \gamma^0\,. \tag{23}$$

In subsequent chapters, we will use the equality

$$\bar{u}_f \not{q} u_i = 0\,, \tag{24}$$

which follows directly from the Dirac equation (19). Keep in mind that every statement here is made without being restrained to any particular base or representation.

4.2 Leptons

At this point, we might wonder what the amplitude of elastic lepton-lepton scattering looks like. So, for once we will consider a lepton (e.g. an electron or muon) as the target as well,

$$l_{\text{target}}(p_i) + l_{\text{beam}}(k_i) \to l_{\text{target}}(p_f) + l_{\text{beam}}(k_f)\,. \tag{25}$$

A particularly elegant way to formulate the amplitude is with Feynman rules. To illustrate this, we will deviate from the procedure in Chapter 2.1. For our purposes, we only need the rules listed in Table 1.

For every ...	draw ...	write ...
Incoming lepton		$u(p)$
Outgoing lepton		$\bar{u}(p)$
Internal photon line		$\dfrac{-ig_{\mu\rho}}{q^2}$
Vertex		$-ie\gamma^\mu$

Table 1: Selection of Feynman rules relevant to leading order QED processes of elastic lepton scattering.

Applying the Feynman rules onto the Feynman diagram of process (25) and reflecting onto its hermitian yields Figure 6.

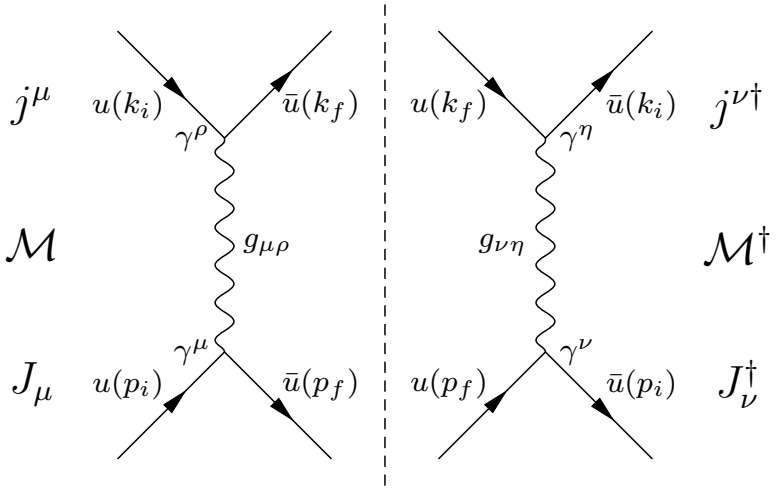

Figure 6: The Feynman diagram of the $l(p_i)+l(k_i) \to l(p_f)+l(k_f)$ scattering process including its hermitian reflection.

The amplitude is then formed by placing the terms in the Feynman rules in the appropriate order,

$$\begin{aligned}\mathcal{M} &= (-i)\bar{u}(p_f)(-ie\gamma^\mu)u(p_i)\Big[\frac{-ig_{\mu\rho}}{(p_f-p_i)^2}\Big]\bar{u}(k_f)(-ie\gamma^\rho)u(k_i) \\ &= -\frac{e^2}{q^2}[\bar{u}(p_f)\gamma^\mu u(p_i)][\bar{u}(k_f)\gamma_\mu u(k_i)] \\ &= -\frac{e^2}{q^2}J^\mu j_\mu\,,\end{aligned} \tag{26}$$

where we isolate the electromagnetic current of the target lepton,

$$J_\mu = \bar{u}(p_f)\gamma_\mu u(p_i)\,. \tag{27}$$

Notice that in the spirit of the argument we are handling the beam lepton in LO as well. We must not forget that in practice, NNLO corrections have to be applied to the beam. However, this simplification does not affect the important calculations performed here.

Taking the absolute square of the amplitude, we may regroup terms with high and low indices together,

$$\begin{aligned}|\mathcal{M}|^2 = \mathcal{M}\mathcal{M}^\dagger &= \frac{e^4}{q^4}\Big(J_\mu j^\mu\Big)\Big(J_\nu j^\nu\Big)^\dagger \\ &= \frac{e^4}{q^4}(J_\mu J_\nu^\dagger)(j^\mu j^{\nu\dagger}) \\ &= \frac{e^4}{q^4}H_{\mu\nu}L^{\mu\nu}\,.\end{aligned} \tag{28}$$

This gives us the "hadronic" tensor of the target lepton

$$H_{\mu\nu} = [\bar{u}_f\gamma_\mu u_i][\bar{u}_i\gamma_\nu u_f]\,, \tag{29}$$

where we from now on omit the notion of the momentum p, e.g. by writing $u(p_i) = u_i$. We can compute the unpolarised hadronic tensor by using the completeness relation (22) in steps 3 and 4. Afterwards, we restore the implicit spinor indices to introduce the trace.

$$\begin{aligned}H_{\mu\nu}^{(0)} &= \frac{1}{2}\sum_{\text{spin out}}\sum_{\text{spin in}}H_{\mu\nu} \\ &= \frac{1}{2}\sum_{\lambda_f}\sum_{\lambda_i}\big[\bar{u}_f\gamma_\mu u_i\bar{u}_i\gamma_\nu u_f\big] \\ &= \frac{1}{2}\sum_{\lambda_f}\bar{u}_f\big[\gamma_\mu(\not{p}_i+m)\gamma_\nu\big]u_f \\ &= \frac{1}{2}\mathrm{Tr}\big(\gamma_\mu(\not{p}_i+m)\gamma_\nu(\not{p}_f+m)\big) \\ &= 2\big[(p_i)_\mu(p_f)_\nu + (p_i)_\nu(p_f)_\mu + (m^2 - p_i\cdot p_f)g_{\mu\nu}\big]\,.\end{aligned} \tag{30}$$

The trace can be computed either by utilising properties of the Gamma matrices, or with Package-X. Details can be found in numerous texts, whereupon [12] provides a particularly detailed calculation.

The other possibility is to maintain the spinors and explicitly sum over all possible helicity states. In that case, we directly get

$$\begin{aligned} H_{\mu\nu}^{(0)} = \frac{1}{2}\Big(& [\bar{u}_f^+ \gamma_\mu u_i^+][\bar{u}_i^+ \gamma_\nu u_f^+] + [\bar{u}_f^- \gamma_\mu u_i^-][\bar{u}_i^- \gamma_\nu u_f^-] \\ & + [\bar{u}_f^+ \gamma_\mu u_i^-][\bar{u}_i^- \gamma_\nu u_f^+] + [\bar{u}_f^- \gamma_\mu u_i^+][\bar{u}_i^+ \gamma_\nu u_f^-] \Big) , \end{aligned} \tag{31}$$

where the $\pm$-sign reflects the $\pm 1/2$-spin state of the spinors.

4.2.1 Numerical comparison

To reiterate, everything previously mentioned works in any representation, as long as the γ-matrices satisfy the Dirac algebra (20). For the numerical part, we choose the Dirac representation of the γ-matrices which depends on the Pauli matrices. This can be found in any standard text, such as [13].

For the Dirac spinors, we use the classic representation

$$u^+ = \frac{1}{\sqrt{E+m}} \begin{pmatrix} E+m \\ 0 \\ p_z \\ p_x + i p_y \end{pmatrix} \quad \text{and} \quad u^- = \frac{1}{\sqrt{E+m}} \begin{pmatrix} 0 \\ E+m \\ p_x - i p_y \\ -p_z \end{pmatrix} . \tag{32}$$

We utilised the test momenta (10) in the numerical illustration. To calculate the unpolarised hadronic tensor, both the computed trace (30) and the helicity sum (31) yield the same result,

$$H_{\mu\nu}^{(0)} = \begin{pmatrix} 270 & -10 & -22 & -246 \\ -10 & 10 & 28 & 4 \\ -22 & 28 & 82 & 16 \\ -246 & 4 & 16 & 258 \end{pmatrix} . \tag{33}$$

This is a numerical demonstration of the equality

$$\begin{aligned} H_{\mu\nu}^{(0)} &= \frac{1}{2} \sum_{\lambda_f = \pm 1/2} \sum_{\lambda_i = \pm 1/2} [\bar{u}_f^{\lambda_f} \gamma_\mu u_i^{\lambda_i}][\bar{u}_i^{\lambda_i} \gamma_\nu u_f^{\lambda_f}] \\ &= 2(p_i)_\mu (p_f)_\nu + 2(p_i)_\nu (p_f)_\mu + Q^2 g_{\mu\nu} . \end{aligned} \tag{34}$$

4.3 Hadrons

If we replace the point-like lepton with a more complex spin 1/2 particle, say, a proton, we must drop the pretence of the point charge distribution. To accurately describe its electromagnetic charge distribution and thus its behaviour in the scattering process, we must leave the Feynman rules at the door and return to the general approach described in Chapter 2.1.

Compared to the scalar case, we have four-dimensional vectors as spinors, so we better have 4×4 matrices in the vertex. The exhaustive list of objects that can appear limit to p_i^μ, p_f^μ, and γ^μ, which can be obtained by expanding Γ^μ in the 16 covariant matrices [14]. Similarly to (11) we consider the general linear combination, which we may rewrite as

$$\Gamma^\mu = A\gamma^\mu + B(p_f + p_i)^\mu + C(p_f - p_i)^\mu \,. \tag{35}$$

Here, p_i^μ and p_f^μ, which are scalars in the spinor space for a fixed Lorentz index, are understood to be multiplied by the 4-dimensional unit matrix. By (5),

$$q_\mu\big(\bar{u}_f \Gamma^\mu u_i\big) = A\bar{u}_f \not{q} u_i + B(p_f^2 - p_i^2)\bar{u}_f u_i + Cq^2 \bar{u}_f u_i \overset{!}{=} 0 \,, \tag{36}$$

we notice that the first term vanishes by (24). The second term disappears after contraction with q, since $p_f^2 = p_i^2 = m^2$. The third term does not automatically vanish, so we set $C = 0$. Via the Gordon identity (cf. [15]) and reparametrisations $F_1 = A + 2mB$ and $F_2 = -2mB$, we arrive at the vertex

$$\Gamma^\mu = \gamma^\mu F_1(Q^2) + \frac{i\sigma^{\mu\{q\}}}{2m} F_2(Q^2) \,, \tag{37}$$

with the notation $\sigma^{\mu\{q\}} = \sigma^{\mu\nu} q_\nu$. F_1 and F_2 are the electric monopole and magnetic dipole form factors, respectively. The current J^μ is then formed by sandwiching Γ^μ between $\bar{u}_f$ and u_i according to (6).

We are now ready to proceed exactly as in the previous chapter, starting at (29), where we just substitute γ_μ with Γ_μ. The trace is evaluated using Package-X,

$$\begin{aligned} H^{(0)}_{\mu\nu} = {} & \big(p_i^\mu p_i^\nu + p_f^\mu p_f^\nu\big)(1-\tau)F_2(Q^2)^2 \\ & + \big(p_f^\nu p_i^\mu + p_f^\mu p_i^\nu\big)\Big(2F_1(Q^2)^2 - (1+\tau)F_2(Q^2)^2\Big) \\ & + g^{\mu\nu}Q^2\big(F_1(Q^2)^2 - F_2(Q^2)^2\big) \,, \end{aligned} \tag{38}$$

where we designate a commonly emerging factor,

$$\tau = \frac{Q^2}{4m^2} \,. \tag{39}$$

Equation (38) is the contracted expression of the unpolarised hadronic tensor for spin 1/2. Notice that for $F_1 \to 1$ and $F_2 \to 0$, we recover the leptonic case (30).

4.3.1 Numerical comparison

We aim to numerically review the equality

$$H^{(0)}_{\mu\nu} = \frac{1}{2}\mathrm{Tr}\big(\Gamma_\mu(\not{p}_i + m)\Gamma_\nu(\not{p}_f + m)\big) = \frac{1}{2}\sum_{\lambda_f=\pm 1/2}\sum_{\lambda_i=\pm 1/2}\left[\bar{u}_f^{\lambda_f}\Gamma_\mu u_i^{\lambda_i}\right]\left[\bar{u}_i^{\lambda_i}\Gamma_\nu u_f^{\lambda_f}\right], \tag{40}$$

where we choose the same representation as in chapter 4.2.1. Indeed, the numerical tensor produces

$$H^{(0)}_{\mu\nu} = \frac{1}{10}\begin{pmatrix} 361 & -19 & -19 & -247 \\ -19 & 1 & 1 & 13 \\ -19 & 1 & 1 & 13 \\ -247 & 13 & 13 & 169 \end{pmatrix} \tag{41}$$

in both computations.

5 Spin 1

At the centre of our endeavours lies the treatment of spin 1-particles. Their prototypical example is the deuteron, which is the nucleus of a heavy hydrogen atom, ${}^2H = d$. The photon as a spin 1-boson is not a fitting example as they do not self-interact. Therefore, we must make use of the massive polarisation vectors ξ_μ.

5.1 Polarisation vector

The fundamental difference between the spin 1-polarisation vectors and the Dirac spinors is that they transform like vectors under the Lorentz group. Analogous to (22), they have a completeness relation of their own,

$$\sum_{\lambda=-1,0,1} \xi_\mu^\lambda (\xi_\nu^\lambda)^* = -g_{\mu\nu} + \frac{p_\mu p_\nu}{m^2} \,. \tag{42}$$

Spin 1-polarisation vectors are four-vectors in the Lorentz space and therefore have one degree of freedom more than would be expected of the three states -1, 0, and 1. Luckily, their orthogonality to their momentum,

$$p^\mu \xi_\mu = 0 \,, \tag{43}$$

provides a constraint to remove one degree of freedom. This property is also called transverse. Another fundamental characteristic of the polarisation vectors is their spin-dependent orthogonality to each other,

$$\xi^{\lambda\mu} (\xi_\mu^{\lambda'})^* = -\delta_{\lambda\lambda'} \,. \tag{44}$$

These attributes generally hold regardless of their representation.

5.2 Derivation of the current

Since the spin functions are Lorentz vectors, the vertex must possess 3 Lorentz indices,

$$J^\mu = \xi_{f_\nu}^* \Gamma^{\mu\nu\rho} \xi_{i_\rho} \,. \tag{45}$$

It is further required for the vertex to be a linear combination of tensors of rank 3, comprising the metric tensor and the momentum vectors. Our ansatz takes the form

$$\Gamma^{\mu\nu\rho} = A_1 g^{\mu\nu} p_f^\rho + A_2 g^{\mu\rho} p_i^\nu + B_1 g^{\nu\rho} p_i^\mu + B_2 g^{\nu\rho} p_f^\mu + C_1 p_i^\mu p_i^\nu p_f^\rho + C_2 p_f^\mu p_i^\nu p_f^\rho \,, \tag{46}$$

as any other possible terms immediately vanish by (43). After contraction,

$$\begin{aligned} q_\mu \big(\xi_{f_\nu}^* \Gamma^{\mu\nu\rho} \xi_{i_\rho}\big) = \frac{1}{2} \Big[& (B_1 - B_2) Q^2 \xi_f^* \cdot \xi_i \\ & + \Big(2\big(A_2 - A_1\big) + \big(C_1 - C_2\big) Q^2 \Big) (\xi_f^* \cdot p_i)(p_f \cdot \xi_i) \Big] \stackrel{!}{=} 0 \,, \end{aligned} \tag{47}$$

we observe that $A_2 = A_1$, $B_2 = B_1$, and $C_2 = C_1$, which produces the current

$$J^\mu = A_1\big(p_f \cdot \xi_i \xi_f^{*\mu} + \xi_f^* \cdot p_i \xi_i^\mu\big) + B_1(\xi_f^* \cdot \xi_i)P^\mu + C_1(\xi_f^* \cdot p_i)(\xi_i \cdot p_f)P^\mu \,. \tag{48}$$

It should be noted that the decision to pair up A_1 with A_2 and C_1 with C_2 is arbitrary. Because of the Q^2-dependence of the coefficients, other pairings (such as $C_2 Q^2 = 2A_2$ and $C_1 Q^2 = 2A_1$) would work as well. We will continue the naive approach of the most obvious pairings, because other pairings are equivalent by reparametrisation.

Similar to Section 3.1, the remaining coefficients are functions of Q^2, which we recognise as form factors. After a reparametrisation of the coefficients, the electromagnetic current for spin 1 takes the form

$$\begin{aligned} J^\mu = P^\mu\Big[-F_1(Q^2)\xi_i \cdot \xi_f^* + \frac{F_3(Q^2)}{m^2}((\xi_i \cdot q)(\xi_f^* \cdot q) + \frac{Q^2}{2}\xi_i \cdot \xi_f^*)\Big] \\ + F_2(Q^2)\big(\xi_i^\mu \xi_f^* \cdot q - \xi_f^{*\mu}\xi_i \cdot q\big)\,, \end{aligned} \tag{49}$$

which is often found in modern literature, such as [16]. This form satisfies the requirements that are Lorentz invariance, current conservation, and parity.

5.3 Computation of the closed form

To derive a closed form of the helicity sum (i.e. without spin functions), consider now

$$H^{(0)}_{\mu\nu} = \frac{1}{3}\sum_{\text{spin out}}\sum_{\text{spin in}} J_\mu J_\nu^* \,. \tag{50}$$

The idea is to explicitly restore the Lorentz indices for all scalar products in (49), expand the complete expression, and then use the completeness relation. In this way, we move the sum into each index pair of spinors, which we replace with the right-hand side of (42). Contracting all spare indices leaves us with

$$\begin{aligned} H^{(0)}_{\mu\nu} = \frac{1}{9}\Big[6\tau F_2(Q^2)^2 + 8\tau^2\big(F_1(Q^2) + F_2(Q^2) + 2F_3(Q^2)\big)^2 \\ + \Big(3F_1(Q^2) + 2\tau\big(F_1(Q^2) + F_2(Q^2) - F_3(Q^2)\big)\Big)^2\Big]P_\mu P_\nu \\ - \frac{2}{3}(\tau+1)F_2(Q^2)^2\big(q_\mu q_\nu + g_{\mu\nu}Q^2\big)\,. \end{aligned} \tag{51}$$

The ξ's have been eliminated, which leaves us with the hadronic tensor corresponding to the case of unpolarised initial and final deuterons.

Additionally, one might want to tidy up (51) by implementing the standard form factors

$$\begin{aligned} G_M(Q^2) &= -F_2(Q^2)\,, \\ G_Q(Q^2) &= F_1(Q^2) + F_2(Q^2) + 2F_3(Q^2)\,, \quad \text{and} \\ G_C(Q^2) &= \frac{2}{3}\tau\Big(F_2(Q^2) - F_3(Q^2)\Big) + \Big(1 + \frac{2}{3}\tau\Big)F_1(Q^2)\,, \end{aligned} \tag{52}$$

where the G_C, G_M, and G_Q represent the form factor for the charge monopole, magnetic dipole, and charge quadrupole, respectively. Furthermore, we can introduce the structure functions

$$\begin{aligned} H_1(Q^2) &= -\frac{2}{3}Q^2(1+\tau)G_M(Q^2)^2 \quad \text{and} \\ H_2(Q^2) &= M^2\Big(G_C(Q^2)^2 + \frac{2}{3}\tau G_M(Q^2)^2 + \frac{8}{9}\tau^2 G_Q(Q^2)^2\Big)\,. \end{aligned} \tag{53}$$

Following [16], this leaves us with a compact formulation of the unpolarised hadronic spin 1-tensor,

$$H^{(0)}_{\mu\nu} = H_1(Q^2)\Big(g_{\mu\nu} + \frac{q_\mu q_\nu}{Q^2}\Big) + H_2(Q^2)\frac{P_\mu P_\nu}{m^2}\,. \tag{54}$$

5.4 Numerical comparison

We choose the adjoint representation of a spin 1-particle, particularly of its spin operator. Its eigenvalues -1, 0, and 1 represent the three spin states. Their corresponding eigenvectors are

$$\vec{e}_{-1} = \frac{1}{\sqrt{2}}\begin{pmatrix}1\\-i\\0\end{pmatrix}, \quad \vec{e}_0 = \begin{pmatrix}0\\0\\1\end{pmatrix}, \quad \text{and} \quad \vec{e}_1 = \frac{1}{\sqrt{2}}\begin{pmatrix}-1\\-i\\0\end{pmatrix}, \tag{55}$$

which describe the polarisation vector in its rest frame. Boosting them yields the general form,

$$\xi^\mu(p,\lambda) = \left(\frac{\vec{p}\cdot\vec{e}_\lambda}{m}, \vec{e}_\lambda + \frac{\vec{p}\cdot\vec{e}_\lambda}{m(E+m)}\vec{p}\right). \tag{56}$$

Analogously to (34) and (40), we aim to check the identity (50). In this case, the two computations produce the tensor

$$H^{(0)}_{\mu\nu} = \frac{1}{225}\begin{pmatrix} 388816 & -20064 & -21204 & -271852 \\ -20064 & 1956 & 3666 & 13458 \\ -21204 & 3666 & 8796 & 14598 \\ -271852 & 13458 & 14598 & 194524 \end{pmatrix}. \tag{57}$$

6 Spin 3/2

Spin 3/2-particles are less discussed than particles of spin 0, 1/2, and 1, as they emerge less frequently. Examples include members of the uds baryon decuplet and several nuclides, such as ^{197}Au, the only stable gold isotope [17].

6.1 Interlude: spin coupling and Clebsch-Gordan decomposition

The formulation of spin functions for higher spin can be achieved by coupling spinors of lower spin together. If one desires a spin function of spin j, then one must couple spin functions of spin j_1 and j_2 together, such that $j_1 + j_2 = j$. The Clebsch-Gordan decomposition provides the necessary coefficients, which can be directly calculated or looked up at [18]. However, the general formula for this procedure,

$$j_1 \otimes j_2 = \bigoplus_{s=|j_1-j_2|}^{j_1+j_2} s\,, \tag{58}$$

already creates complications. Apart from spin j, which is what we desire, the coupling also produces terms of lower spin (namely $j-1, j-2, \ldots, |j_1 - j_2|$). The problem at hand is that this coupled state initially has more degrees of freedom (d.o.f.) than we would expect.

Generally, a spin function of spin j has $2j+1$ d.o.f., one per spin configuration. Since the degrees of freedom are multiplied in the direct product and added up in the direct sum, we see that our coupled state initially has $4j_1j_2$ d.o.f. too much. We thus need a way to reduce excess degrees by finding constraints.

6.2 Polarisation vector

To distinguish from the Dirac spinors u and anti-spinors v, we denote w to be the spin function. We formulate spin 3/2 in the combination

$$\frac{1}{2} \otimes 1 = \frac{3}{2} \oplus \frac{1}{2}\,. \tag{59}$$

By the Clebsch Gordan-decomposition, spin 3/2-functions are of the form [19]

$$\begin{aligned} w_\mu^{\pm 3/2} &= u^\pm \xi_\mu^{\pm 1} \quad \text{and} \\ w_\mu^{\pm 1/2} &= \frac{1}{\sqrt{3}} u^\mp \xi_\mu^{\pm 1} + \sqrt{\frac{2}{3}} u^\pm \xi_\mu^0\,. \end{aligned} \tag{60}$$

This leaves us with $2 \cdot 4 = 8$ degrees of freedom, of which four must be eliminated. Luckily, there are four constraints to work with,

$$p^\mu w_\mu = 0 \quad \text{and} \quad \gamma^\mu w_\mu = 0\,. \tag{61}$$

In other words, spin 3/2-functions are transverse and can be covariantly eliminated. Each equation accounts for two constraints, as they hold for both states of the Dirac spinor component.

Furthermore, they satisfy the Dirac equation,

$$(\not{p} - m)w^\mu = 0\,, \tag{62}$$

and their completeness relation is of the form [20]

$$\sum_{\lambda=\pm 3/2,\pm 1/2} w_\mu^\lambda \bar{w}_\nu^\lambda = -(\not{p} + m)\Big[g_{\mu\nu} - \frac{1}{3}\gamma_\mu\gamma_\nu - \frac{2}{3m^2}p_\mu p_\nu - \frac{1}{3m}(\gamma_\mu p_\nu - \gamma_\nu p_\mu)\Big]\,. \tag{63}$$

The adjoint spinor $\bar{w}$ is formed similarly to (60) by combining the Dirac adjoint $\bar{u}$ and the complex conjugate polarisation vector ξ_μ^*. We denote the quantity in (63) as $\Pi_{\mu\nu}(p)$, since we will need it later.

6.3 Derivation of the current

By employing all combinations of allowed objects (similar to Chapter 4.3), the ansatz for the vertex is

$$\begin{aligned}\Gamma^{\mu\nu\rho} = {} & A_1\gamma^\mu g^{\nu\rho} + A_2\gamma^\mu p_i^\nu p_f^\rho \\ & + B_1 p_i^\mu g^{\nu\rho} + B_2 p_f^\mu g^{\nu\rho} + B_3 p_i^\nu g^{\mu\rho} + B_4 p_f^\rho g^{\mu\nu} \\ & + C_1 p_i^\mu p_i^\nu p_f^\rho + C_2 p_i^\nu p_f^\mu p_f^\rho\,.\end{aligned} \tag{64}$$

Again, we understand terms without γ^μ to be multiplied by the unit matrix. Due to the constraints (61) of w, these are the only terms which do not immediately vanish. The covariant elimination in particular is accountable for the lack of any terms containing γ^ν and γ^ρ. An exemplary calculation goes as follows:

$$\begin{aligned}\bar{w}_\nu\gamma^\rho\gamma^\mu\gamma^\nu w_\rho &= \bar{w}_\nu(2g^{\rho\mu} - \gamma^\mu\gamma^\rho)\gamma^\nu w_\rho = -\bar{w}_\nu\gamma^\mu\gamma^\rho\gamma^\nu w_\rho \\ &= -\bar{w}_\nu\gamma^\mu(2g^{\rho\nu} - \gamma^\nu\gamma^\rho)w_\rho = \bar{w}_\nu\big[A_1\gamma^\mu g^{\nu\rho}\big]w_\rho\,.\end{aligned} \tag{65}$$

Any other combination can similarly be reduced to an already existing term in (64). For the vertex to satisfy gauge invariance, we require

$$q_\mu \bar{w}_{f_\nu}\Gamma^{\mu\nu\rho}w_{i\rho} \stackrel{!}{=} 0\,, \tag{66}$$

from which we infer $B_2 = B_1$, $B_4 = B_3$, and $C_2 = C_1$. The A_1 and A_2 terms vanish by (24). Suspicion should arise due to the number of remaining coefficients, which is one more than expected. We will return to this issue in Chapter 8.2. To that end, one can show (e.g. with Package-X) that the vertex is equivalent to

$$\begin{aligned}\Gamma^{\mu\nu\rho} = {} & \big(A_1 g^{\nu\rho} + A_2 p_i^\nu p_f^\rho + 2B_1 m g^{\nu\rho} + 2C_1 m p_i^\nu p_f^\rho\big)\gamma^\mu \\ & - i\big(B_1 g^{\nu\rho} + C_1 p_i^\nu p_f^\rho\big)\sigma^{\mu\{q\}} + \big(p_i^\nu g^{\mu\rho} + p_f^\rho g^{\mu\nu}\big)B_3\,.\end{aligned} \tag{67}$$

Following the same logic as in (30), we compute the unpolarised hadronic tensor,

$$\begin{aligned} H^{(0)}_{\mu\nu} &= \frac{1}{4}\sum_{\text{spins}} J_\mu J^\dagger_\nu \\ &= \frac{1}{4}\sum_{\text{spins}} \left[\bar{w}_{f_\eta}\Gamma^{\mu\eta\rho} w_{i\rho}\right]\left[\bar{w}_{i\alpha}\Gamma^{\nu\alpha\beta} w_{f_\beta}\right] \\ &= \mathrm{Tr}\big(\Gamma^{\mu\eta\rho}\Pi_{\rho\alpha}(p_i)\Gamma^{\nu\alpha\beta}\Pi_{\beta\eta}(p_f)\big) \\ &= H_1(Q^2)(p_{i\mu}p_{i\nu} + p_{f_\mu}p_{f_\nu}) + H_2(Q^2)(p_{i\mu}p_{f_\nu} + p_{f_\mu}p_{i\nu}) + H_3(Q^2)g_{\mu\nu}\,, \end{aligned} \tag{68}$$

where the coefficients have been truncated to structure functions H_1, H_2, and H_3 for brevity.

7 Spin 2

The territory of spin 2-particles is less well explored than any spin before, as their representatives are mainly exotic. One such example is the hypothetical, massless, and uncharged graviton. It is postulated to be the gauge boson for gravity interactions and would possess spin 2. However, it is not very well suited as the target of a scattering experiment, for several self-explanatory reasons. More suitable targets are ^{36}Cl and ^{204}Tl [17], which are the only known nuclides to have spin 2. This chapter should thus be considered a mainly theoretical pondering.

7.1 Polarisation tensor

Following the same reasoning as in the previous chapter, we consider the combination

$$1 \otimes 1 = 2 \oplus 1 \oplus 0\,. \tag{69}$$

From this, we can already guess the spin function to be a tensor of rank 2 denoted ζ, which generally indicates 16 degrees of freedom. By the Clebsch-Gordan decomposition, the spin 2 functions are of the form

$$\begin{aligned} \zeta^{\pm 2}_{\mu\nu} &= \xi^{\pm 1}_{\mu}\xi^{\pm 1}_{\nu}\,, \\ \zeta^{\pm 1}_{\mu\nu} &= \frac{1}{\sqrt{2}}(\xi^{\pm 1}_{\mu}\xi^{0}_{\nu} + \xi^{0}_{\mu}\xi^{\pm 1}_{\nu})\,, \quad \text{and} \\ \zeta^{0}_{\mu\nu} &= \frac{1}{\sqrt{6}}(\xi^{1}_{\mu}\xi^{-1}_{\nu} + \xi^{-1}_{\mu}\xi^{1}_{\nu} + 2\xi^{0}_{\mu}\xi^{0}_{\nu})\,. \end{aligned} \tag{70}$$

ζ needs to be a symmetric and traceless tensor,

$$\zeta_{\mu\nu} = \zeta_{\nu\mu} \quad \text{and} \quad \zeta_{\mu\nu}g^{\mu\nu} = 0\,, \tag{71}$$

which removes six and one d.o.f., respectively. It can be easily checked that these conditions are met by the coupled states (70). The last four redundant d.o.f. are omitted by transversity,

$$p^{\mu}\zeta_{\mu\nu}\,, \tag{72}$$

since this holds independently for every ν index.

Similar to spin 1, spin 2-functions are orthonormal,

$$\zeta^{\lambda\mu\nu}(\zeta^{\lambda'}_{\mu\nu})^{*} = \delta_{\lambda\lambda'}\,, \tag{73}$$

and fulfill the completeness relation [21],

$$\sum_{\lambda=-2,\dots,2} \zeta^{\lambda}_{\mu\nu}(\zeta^{\lambda}_{\rho\eta})^{*} = \frac{1}{2}\left(g_{\mu\rho} - \frac{p_\mu p_\rho}{m^2}\right)\left(g_{\eta\nu} - \frac{p_\nu p_\eta}{m^2}\right) + \frac{1}{2}\left(g_{\eta\mu} - \frac{p_\mu p_\eta}{m^2}\right)\left(g_{\nu\rho} - \frac{p_\nu p_\rho}{m^2}\right) \tag{74}$$

$$-\frac{1}{3}\left(g_{\mu\nu} - \frac{p_\mu p_\nu}{m^2}\right)\left(g_{\eta\rho} - \frac{p_\rho p_\eta}{m^2}\right)\,. \tag{75}$$

7.2 Derivation of the current

Taking transversity and tracelessness into account, the naive ansatz of the vertex contains 26 terms. However, because the current is formed after contracting the vertex with $\zeta_{\rho_1\rho_2}(p_i)$ and $\zeta_{\nu_1\nu_2}(p_f)^*$, we can reduce the form of the vertex further with the aid of additional symmetry considerations. The symmetry of ζ implies that the vertex is symmetric in the second and third, and in the fourth and fifth argument, respectively, i.e. $\Gamma^{\mu\nu_1\nu_2\rho_1\rho_2} = \Gamma^{\mu\nu_2\nu_1\rho_1\rho_2} = \Gamma^{\mu\nu_1\nu_2\rho_2\rho_1} = \Gamma^{\mu\nu_2\nu_1\rho_2\rho_1}$. Grouping together terms with such a particular symmetry yields

$$\begin{aligned}
\Gamma^{\mu\nu_1\nu_2\rho_1\rho_2} =& A_1 p_i^\mu p_i^{\nu_1} p_i^{\nu_2} p_f^{\rho_1} p_f^{\rho_2} + A_2 p_i^{\nu_1} p_i^{\nu_2} p_f^{\rho_1} p_f^{\rho_2} p_f^\mu \\
&+ B_1 p_i^\mu \left[g^{\rho_1\nu_2} g^{\rho_2\nu_1} + g^{\rho_1\nu_1} g^{\rho_2\nu_2} \right] + B_2 p_f^\mu \left[g^{\rho_1\nu_2} g^{\rho_2\nu_1} + g^{\rho_1\nu_1} g^{\rho_2\nu_2} \right] \\
&+ C_1 p_i^{\nu_1} p_i^{\nu_2} \left[p_f^{\rho_2} g^{\rho_1\mu} + p_f^{\rho_1} g^{\rho_2\mu} \right] + C_2 p_f^{\rho_1} p_f^{\rho_2} \left[p_i^{\nu_2} g^{\mu\nu_1} + p_i^{\nu_1} g^{\mu\nu_2} \right] \\
&+ D_1 p_i^\mu \left[p_i^{\nu_2} p_f^{\rho_2} g^{\rho_1\nu_1} + p_i^{\nu_1} p_f^{\rho_2} g^{\rho_1\nu_2} + p_i^{\nu_2} p_f^{\rho_1} g^{\rho_2\nu_1} + p_i^{\nu_1} p_f^{\rho_1} g^{\rho_2\nu_2} \right] \\
&+ D_2 p_f^\mu \left[p_i^{\nu_2} p_f^{\rho_2} g^{\rho_1\nu_1} + p_i^{\nu_1} p_f^{\rho_2} g^{\rho_1\nu_2} + p_i^{\nu_2} p_f^{\rho_1} g^{\rho_2\nu_1} + p_i^{\nu_1} p_f^{\rho_1} g^{\rho_2\nu_2} \right] \\
&+ E_1 \left[p_i^{\nu_2} \left(g^{\rho_1\nu_1} g^{\rho_2\mu} + g^{\rho_1\mu} g^{\rho_2\nu_1} \right) + p_i^{\nu_1} \left(g^{\rho_1\nu_2} g^{\rho_2\mu} + g^{\rho_1\mu} g^{\rho_2\nu_2} \right) \right] \\
&+ E_2 \left[p_f^{\rho_2} \left(g^{\rho_1\nu_2} g^{\mu\nu_1} + g^{\rho_1\nu_1} g^{\mu\nu_2} \right) + p_f^{\rho_1} \left(g^{\rho_2\nu_2} g^{\mu\nu_1} + g^{\rho_2\nu_1} g^{\mu\nu_2} \right) \right],
\end{aligned} \tag{76}$$

which leaves us with 10 terms. Following the same procedure as before, we contract $\Gamma^{\mu\nu_1\nu_2\rho_1\rho_2}$ with $\zeta_{\rho_1\rho_2}(p_i)$, $\zeta_{\nu_1\nu_2}(p_f)^*$, and q_μ, requiring this quantity to vanish. The naive substitution here is $A_2 = A_1$, $B_2 = B_1$, $C_2 = C_1$, $D_2 = D_1$, and $E_2 = E_1$. Omitting constant factors, the proposed form of the current becomes

$$\begin{aligned}
J^\mu =& A_1 P^\mu \zeta_i^{\{p_f\}\{p_f\}} (\zeta_f^{\{p_i\}\{p_i\}})^* + B_1 P^\mu \zeta_i^{\alpha\beta} (\zeta_{f\,\alpha\beta})^* \\
&+ C_1 \left(\zeta_i^{\mu\{p_f\}} (\zeta_f^{\{p_i\}\{p_i\}})^* + \zeta_i^{\{p_f\}\{p_f\}} (\zeta_f^{\mu\{p_i\}})^* \right) \\
&+ D_1 P^\mu \zeta_i^{\alpha\{p_f\}} (\zeta_{f\,\alpha}^{\{p_i\}})^* + E_1 \left(\zeta_i^{\mu\alpha} (\zeta_{f\,\alpha}^{\{p_i\}})^* + \zeta_i^{\alpha\{p_f\}} (\zeta_{f\,\alpha}^{\mu})^* \right),
\end{aligned} \tag{77}$$

with the notation convention

$$\zeta^{\mu\{p\}} = \zeta^{\mu\alpha} p_\alpha \quad \text{and} \quad \zeta^{\{p\}\{p'\}} = \zeta^{\alpha\beta} p_\alpha p'_\beta \,. \tag{78}$$

It is now possible to compute the hadronic tensor exactly as before, either by (a) replacing the spin 2-functions in terms of their completeness relation (74), or (b) explicitly summing over the incoming and outgoing spins.

8 Spin $n/2$

The general description of the spin functions was provided by Auvil and Brehm in 1966 [22]. In 2009, Lorcé further postulated the form of the electromagnetic current for arbitrary spin [23]. To compare our more heuristic approach with the generalised version, we will follow the two publications closely.

8.1 General formula for integer spin

We return to a more common notation and denote $\xi_{\alpha_1\cdots\alpha_j}(p,\lambda)$ to be the integer spin j-function of momentum p and helicity λ. Applying the Clebsch-Gordan decomposition recursively gives us the general expression

$$\xi_{\alpha_1\cdots\alpha_j}(p,\lambda) = \sum_{m=0,\pm1} \sum_{m'=-j+1}^{j-1} \langle j-1, m_1; 1, m_2 | j, \lambda\rangle \xi_{\alpha_1\cdots\alpha_{j-1}}(p,m_1)\xi_{\alpha_j}(p,m_2)\,. \tag{79}$$

This polarisation tensor is transverse and traceless,

$$p^\mu \xi_{\mu\alpha_2\cdots\alpha_j}(p,\lambda) = 0 \quad \text{and} \quad \xi^\mu_{\mu\alpha_3\cdots\alpha_j}(p,\lambda) = 0\,, \tag{80}$$

which leaves us with $2j+1$ degrees of freedom due to the symmetry of the tensor in every index. The current assumes the form

$$J^\mu = (-1)^j\, \xi^*_{\nu_1\cdots\nu_j}(p_f,\lambda_f) \left[P^\mu \sum_{(k,j)} F_{2k+1}(Q^2) + (g^{\mu\rho_j} q^{\nu_j} - g^{\nu_j\mu} q^{\rho_j}) \sum_{(k,j-1)} F_{2k+2}(Q^2) \right] \xi_{\rho_1\cdots\rho_j}(p_i,\lambda_i), \tag{81}$$

with the introduced notation

$$\sum_{(k,j)} \equiv \sum_{k=0}^{j} \left[\prod_{i=1}^{k} \left(-\frac{q^{\nu_i} q^{\rho_i}}{2m^2} \right) \prod_{i=k+1}^{j} g^{\nu_i\rho_i} \right], \tag{82}$$

and convention $\prod_{i=x}^{x-1} f(i) \equiv 1$. The form factors denote the different electromagnetic multipoles, with odd labels describing electric and even labels describing magnetic multipoles.

We will now compare the vertices for the different spins in (81) with the ones we derived earlier. The expressions agree trivially for spin 0 (14). For spin 1 (48) and spin 2 (77), the expressions coincide almost exactly as well, differing only by constant factors and differently labelled coefficients/form factors.

8.2 General formula for half-integer spin

The half-integer spin j-function with $j = l + 1/2$ of momentum p and helicity λ is denoted by $u_{\alpha_1\cdots\alpha_l}(p,\lambda)$ and assumes the form

$$u_{\alpha_1\cdots\alpha_l}(p,\lambda) = \sqrt{\frac{l+\lambda}{2l}}\, u^+(p)\, \xi_{\alpha_1\cdots\alpha_l}(p,\lambda-\frac{1}{2}) + \sqrt{\frac{l-\lambda}{2l}}\, u^-(p)\, \xi_{\alpha_1\cdots\alpha_l}(p,\lambda+\frac{1}{2})\,. \tag{83}$$

Similar to the integer case, the half-integer spin function is symmetric, transverse, and traceless. It satisfies the additional requirements

$$\big(\not{p} - m\big) u_{\alpha_1\cdots\alpha_l}(p,\lambda) = 0 \quad \text{and} \quad \gamma^\mu u_{\mu\alpha_2\cdots\alpha_l}(p,\lambda) = 0\,, \tag{84}$$

to constitute the right amount of degrees of freedom. The current is of the form

$$J^\mu = (-1)^l\, \bar{u}_{\nu_1\cdots\nu_l}(p_f,\lambda_f) \sum_{(k,l)} \left[\gamma^\mu\, F_{2k+1}(Q^2) + \frac{i\sigma^{\mu\{q\}}}{2m}\, F_{2k+2}(Q^2)\right] u_{\rho_1\cdots\rho_l}(p_i,\lambda_i)\,, \tag{85}$$

with the usual convention (82).

The vertex for spin 1/2 (37) agrees with the general formula. For spin 3/2, we uncover the first real discrepancy between the literature and our previously pursued methodology. The general formula proposes for spin 3/2 the vertex

$$\begin{aligned}\Gamma^{\mu\nu\rho} =& \Big(-F_1(Q^2) g^{\nu\rho} + \frac{F_3(Q^2)}{2m^2}\big(p_f^\nu - p_i^\nu\big)\big(p_f^\rho - p_i^\rho\big)\Big)\gamma^\mu \\ &+ \Big(-F_2(Q^2) g^{\nu\rho} + \frac{F_4(Q^2)}{2m^2}\big(p_f^\nu - p_i^\nu\big)\big(p_f^\rho - p_i^\rho\big)\Big)\frac{i\sigma^{\mu\{q\}}}{2m}\,.\end{aligned} \tag{86}$$

It is easy to see that this expression can mostly be converted to and from (67), apart from the B_3 term. Furthermore, inspecting (85) reveals that this theory does not allow for $g^{\mu\rho}$ and $g^{\mu\nu}$ terms (only $g^{\nu\rho}$ terms are allowed), which are precisely the B_3 and B_4 terms in the ansatz (64). Given that the naive ansatz does not produce the correct amount of form factors, it is likely that the general equation is more accurate. Notice that the ban of metric tensors containing the μ index holds only for half-integer cases, which is why the comparison in the integer case was generally succesful.

9 Conclusion

9.1 Summary

In this thesis, we have considered the first five spin types, which are summarised in Table 2. For spin j functions, the vertex Γ possesses in general $2\lfloor j \rfloor + 1$ Lorentz indices. If j is an integer, Γ is scalar in the spinor space but a true tensor in the Lorentz space. If j is a half-integer, the vertex is a 4×4-matrix in the spinor space but not a Lorentz tensor due to the nature of the γ-matrices.

	Prototypical	Spin function	Lorentz type of Γ	Spinor type of Γ
Spin 0	Carbon ^{12}C	1	vector	scalar
Spin 1/2	Proton p	u	1 Lorentz index	4×4-matrix
Spin 1	Deuteron d	ξ^μ	rank 3-tensor	scalar
Spin 3/2	$\Delta^{++}(1232)$	$u \otimes \xi^\mu$	3 Lorentz indices	4×4-matrix
Spin 2	Chlorine ^{36}Cl	$\xi^\mu \otimes \xi^\nu$	rank 5-tensor	scalar

Table 2: Summary of the spin types considered and the resulting mathematical structure of the vertex Γ.

A question that arose in the naive approach was the number of expected terms in the electromagnetic current. Because of their dependence on Q^2, the elimination of coefficients to satisfy gauge invariance is not unique, and there are sometimes more degrees of freedom than expected, as is the case with spin 3/2. The pairing of coefficients presented here was intuitive, but not substantially founded. The exact nature of resolving this question is currently open.

Furthermore, how to generally link the arising coefficients to physical form factors or structure functions such as in (52) and (53) is ambiguous and depends on the conventions used by authors or research groups in the literature. For example, various expressions for the electromagnetic current of spin 1 have been uncovered, most of them were equivalent by reparametrisation but not identical.

Literature of the general procedure of producing electromagnetic currents associated with the hadronic target was discovered in the late stage of writing this thesis. For this reason, a closer examination of the methodology described was not possible. It was however within scope to cross-examine the results harvested by the naive method with the methodology in the paper. This solidified correct results and at least partially explained some discrepancies, where present. In-depth discussion surrounding the publication including electromagnetic multipole decomposition can be found in [24, 25, 26, 27].

9.2 Outlook

There are many different prospects and motivations to generalise the formulation of the transition current in the same manner as in (81) and (85). One possibility is to consider amplitudes which include radiative corrections on the hadronic side as well, which can be applied to future simulations of Muse experiments [28]. The second prospect is to branch out towards amplitudes which arise in electroweak interactions. There are ongoing efforts made for McMule to be able to carry out such calculations in the future. This can then be implemented to simulate the P2 experiment [29], amongst others.

At present, McMule is able to perform calculations of $2 \to 2$ processes at NNLO. The next logical step is to expand to calculating $2 \to 3$ processes, such as the one discussed in Chapter 3.2, at NNLO as well. OpenLoops, which currently operates at one-loop, gets extended as well. This is needed for numerically stable evaluation of two-loop amplitudes, which then can get implemented into McMule. Finally, the involvement of McMule with ULQ2 promises to be an exciting avenue on the precision frontier, for both experimental and theoretical developments.

References

[1] M. Mihovilovič et al. "First measurement of proton's charge form factor at very low Q2 with initial state radiation". In: *Physics Letters B* 771 (Aug. 2017), pp. 194–198. ISSN: 0370-2693. DOI: 10.1016/j.physletb.2017.05.031.

[2] Randolf Pohl et al. "The size of the proton". In: 466.7303 (July 2010), pp. 213–216. DOI: 10.1038/nature09250.

[3] Toshimi Suda. "Low-energy electron scattering facilities in Japan". In: *Journal of Physics: Conference Series* 2391 (Dec. 2022), p. 012004. DOI: 10.1088/1742-6596/2391/1/012004.

[4] Pulak Banerjee et al. "QED at NNLO with McMule". In: *SciPost Phys.* 9 (2020), p. 027. DOI: 10.21468/SciPostPhys.9.2.027. arXiv: 2007.01654 [hep-ph].

[5] Fangcheng He and P. Wang. *Pauli form factors of electron and muon in nonlocal quantum electrodynamics*. 2019. arXiv: 1901.00271 [hep-ph].

[6] W. R. Theis. "Electromagnetic form factors for arbitrary spin". In: *Il Nuovo Cimento A* 45 (1966), pp. 124–144. ISSN: 1826-9869. DOI: 10.1007/BF02738080.

[7] H. H. Patel. "Package-X: A Mathematica package for the analytic calculation of one-loop integrals". In: *Comput. Phys. Commun.* 197 (2015), pp. 276–290. DOI: 10.1016/j.cpc.2015.08.017.

[8] H. H. Patel. "Package-X 2.0: A Mathematica package for the analytic calculation of one-loop integrals". In: *Comput. Phys. Commun.* 218 (2017), pp. 66–70. DOI: 10.1016/j.cpc.2017.04.015.

[9] M. Mihovilovič et al. *Non-forward radiative corrections to electron-carbon scattering*. 2023. arXiv: 2303.12196 [hep-ph].

[10] Federico Buccioni, Stefano Pozzorini, and Max Zoller. "On-the-fly reduction of open loops". In: *The European Physical Journal C* 78.1 (Jan. 2018). ISSN: 1434-6052. DOI: 10.1140/epjc/s10052-018-5562-1.

[11] Federico Buccioni et al. "OpenLoops 2". In: *The European Physical Journal C* 79.10 (Oct. 2019). ISSN: 1434-6052. DOI: 10.1140/epjc/s10052-019-7306-2.

[12] M. Sajjad Athar and S. K. Singh. *The Physics of Neutrino Interactions*. Cambridge University Press, 2020, pp. 828–830. ISBN: 978-1-108-48906-5.

[13] Francis Halzen and Alan D. Martin. *Quarks & Leptons: An Introductory Course in Modern Particle Physics*. John Wiley & Sons, Inc., 1984, pp. 101–102. ISBN: 978-0-471-88741-6.

[14] Steven Weinberg. *The Quantum Theory of Fields, Volume 1: Foundations*. Cambridge University Press, 1995, p. 454. ISBN: 0-521-55001-7.

[15] Michael E. Peskin and Daniel V. Schroeder. *An Introduction to Quantum Field Theory*. Westview Press, 1995, p. 186. ISBN: 978-0-201-50397-5.

[16] G. I. Gakh et al. "Polarization effects in elastic deuteron-electron scattering". In: *Phys. Rev. C* 109 (6 June 2024), p. 065203. DOI: 10.1103/PhysRevC.109.065203.

[17] International Atomic Energy Agency. *Live Chart of Nuclides*. https://www-nds.iaea.org/. Accessed: 26 August 2024. November 2023.

[18] Particle Data Group. *Clebsch-Gordan Coefficients, Spherical Harmonics, and d Functions*. https://pdg.lbl.gov/2002/clebrpp.pdf. Accessed: 26 August 2024. May 2024.

[19] J. García Ravelo and A. Queijeiro Fontana. "Polarization in the non-leptonic weak decays of spin-3/2 hyperons". In: *Revista Mexicana de Física* 48.4 (Jan. 2002), pp. 307–309. URL: https://rmf.smf.mx/ojs/index.php/rmf/article/view/3068.

[20] N. D. Christensen et al. "Simulating spin- $\frac{3}{2}$ particles at colliders". In: *The European Physical Journal C* 73.10 (Oct. 2013). ISSN: 1434-6052. DOI: 10.1140/epjc/s10052-013-2580-x.

[21] Tanju Gleisberg et al. "Helicity formalism for spin-2 particles". In: *Journal of High Energy Physics* 2003.09 (Sept. 2003), pp. 001–001. ISSN: 1029-8479. DOI: 10.1088/1126-6708/2003/09/001.

[22] P. R. Auvil and J. J. Brehm. "Wave Functions for Particles of Higher Spin". In: *Phys. Rev.* 145 (4 May 1966), pp. 1152–1153. DOI: 10.1103/PhysRev.145.1152.

[23] Cédric Lorcé. *Electromagnetic Properties for Arbitrary Spin Particles: Part 1 — Electromagnetic Current and Multipole Decomposition*. 2009. arXiv: 0901.4199 [hep-ph].

[24] Cédric Lorcé. "Electromagnetic properties for arbitrary spin particles: Natural electromagnetic moments from light-cone arguments". In: *Phys. Rev. D* 79 (11 June 2009), p. 113011. DOI: 10.1103/PhysRevD.79.113011.

[25] Stephan Meißner, Andreas Metz, and Marc Schlegel. "Generalized parton correlation functions for a spin-1/2 hadron". In: *Journal of High Energy Physics* 2009.08 (Aug. 2009), p. 056. DOI: 10.1088/1126-6708/2009/08/056.

[26] Sabrina Cotogno et al. "Covariant multipole expansion of local currents for massive states of any spin". In: *Phys. Rev. D* 101 (5 Mar. 2020), p. 056016. DOI: 10.1103/PhysRevD.101.056016.

[27] E. G. Delgado-Acosta et al. "Electromagnetic multipole moments of elementary spin-1/2, 1, and 3/2 particles". In: *Physical Review D* 85.11 (June 2012). ISSN: 1550-2368. DOI: 10.1103/PhysRevD.85.116006.

[28] T. Engel et al. "Impact of NNLO QED corrections on lepton-proton scattering at MUSE". In: *Eur. Phys. J. A* 59.11 (2023), p. 253. DOI: 10.1140/epja/s10050-023-01153-x. arXiv: 2307.16831 [hep-ph].

[29] Dominik Becker et al. "The P2 experiment: A future high-precision measurement of the weak mixing angle at low momentum transfer". In: *The European Physical Journal A* 54.11 (Nov. 2018). ISSN: 1434-601X. DOI: 10.1140/epja/i2018-12611-6.